Effects of Fermi energy, dot size, and leads width on weak localization in chaotic quantum dots

E. Louis
Departamento de Física Aplicada and Unidad Asociada of the Consejo Superior de Investigaciones Científicas, Universidad de Alicante, Apartado 99, E-03080 Alicante, Spain

J. A. Vergés
Instituto de Ciencia de Materiales de Madrid, Consejo Superior de Investigaciones Científicas, Cantoblanco, E-28049 Madrid, Spain
(Received 5 May 2000; revised manuscript received 27 September 2000; published 27 February 2001)

Magnetotransport in chaotic quantum dots at low magnetic fields is investigated by means of a tight-binding Hamiltonian on $L\times L$ clusters of the square lattice. Chaoticity is induced by introducing L bulk vacancies. The dependence of weak localization on the Fermi energy, dot size, and leads width is investigated in detail and the results compared with those of previous analyses, in particular with random matrix theory predictions. Our results indicate that the dependence of the critical flux Φ_c on the square root of the number of open modes, as predicted by random matrix theory, is obscured by the strong energy dependence of the proportionality constant. Instead, the size dependence of the critical flux predicted by Efetov and random matrix theory, namely, $\Phi_c \propto \sqrt{1/L}$, is clearly illustrated by the present results. Our numerical results do also show that the difference between conductances at large and zero field (weak localization term) significantly decreases as the leads width W approaches L, reaching a value well below the random matrix theory prediction. A size dependence analysis indicates that the weak localization term remains finite when L increases.

DOI: 10.1103/PhysRevB.63.115310 PACS number(s): 73.21.−b, 05.45.−a, 03.65.Sq

I. INTRODUCTION

Experimental studies of magnetoconductance in quantum dots show that, at low magnetic fields (typically below one flux quantum), the conductance increases with the field.[1–4] The effect has been investigated theoretically[2,5,6,8] and related to a similar behavior observed in disordered metallic conductors in the diffusive regime, that is referred to as weak localization (WL).[9,10]

There is also fairly conclusive experimental evidence which indicates that the average magnetoconductance $\langle G(B)\rangle$ behaves in a qualitatively different way in regular and chaotic cavities, namely, whereas in the former it increases linearly with B, in chaotic cavities the WL peak has a Lorentzian shape.[2] Semiclassical analyses ascribe this difference to the different distributions of areas A enclosed by the trajectories of the carriers[5] characteristic of the two cases. While in regular systems the probability distribution of enclosed areas larger than A is $\propto 1/A$,[11] in fully chaotic systems it is exponential.[12] As a consequence, in chaotic cavities the increment in the magnetoconductance as a function of magnetic flux Φ is given by

$$\delta G = G(\Phi) - G(0) = \frac{a\Phi^2}{1+b\Phi^2}, \tag{1}$$

where the conductance and the magnetic flux are given in units of their respective quanta, $G_0 = e^2/h$ and $\Phi_0 = h/e$. The constant b gives the critical flux at which the time-reversal symmetry is effectively destroyed, $\Phi_c = 1/\sqrt{b}$, whereas the ratio a/b gives the weak localization term, i.e., $G(\infty) - G(0) = a/b$. The supersymmetric σ model predicts that a and b should be inversely proportional to the number of channels N_{ch} that contribute to the current,[10]

$$b = c\frac{\nu D_0}{N_{ch}} \propto \frac{L}{N_{ch}}, \tag{2}$$

where c is a constant (for the present geometry $c = 2\pi/3$), ν the density of states, D_0 the diffusion coefficient, and L the linear size of the cavity. The size dependence arises from the standard expression for the diffusion coefficient $D_0 = v_F l/2$, where v_F is the Fermi velocity, and l the elastic mean free path, and from the fact that in a two-dimensional ballistic system, $l \propto L$.[13] The qualitative behavior of Eq. (2) is similar to the random matrix theory (RMT) result for the critical flux at which the time-reversal symmetry is broken (GOE–GUE transition) reported in Ref. 7.

RMT gives the following result for the weak localization term a/b:[8,14,15]

$$\frac{a}{b} = \frac{N_{ch}}{4N_{ch}+2}, \tag{3}$$

where N_{ch} is related to the zero field conductance through

$$G_{\mathrm{RMT}}(0) = \frac{N_{\mathrm{ch}}}{2} - \frac{N_{\mathrm{ch}}}{4N_{\mathrm{ch}}+2}. \tag{4}$$

On the other hand, a fitting of the numerical results obtained from a random matrix model Hamiltonian gave[14]

$$b = 2k\frac{2N_{ch}-1}{N_{ch}^2}, \tag{5}$$

k being a constant which, as in Eq. (2), depends on the Fermi energy. Although Eq. (5) gives the same dependence on the number of channels than Eq. (2) in the large N_{ch} limit, it does not explicitly reproduce neither its size nor its energy dependence. Moreover, as remarked in Ref. 14, Eq. (5) is only valid for few channel ballistic cavities. It should also be

mentioned that the size dependence of the constant b has also been obtained within RMT (see Refs. 16 and 17).

At present there is no published numerical study of the effects of the size of the cavity, the leads width, and the Fermi energy on weak localization in reasonably realistic models of quantum chaotic cavities. The purpose of this work is to discuss the results of such an investigation. Quantum dots are described by means of a tight-binding Hamiltonian on $L\times L$ clusters of the square lattice. Nonregular (chaotic) behavior is induced by introducing a number of bulk vacancies proportional to the linear size of the system.[18] This model has been shown to behave similarly to dots in which chaoticity is induced by introducing disorder at the surface.[19,20] We also note that bulk disorder randomize more efficiently the system than surface disorder making easier the comparison with RMT. The effects of leads width W, system size, and number of channels that contribute to the current are discussed in detail. Our results show that the critical flux is not simply proportional to the square root of the number of open channels as concluded in Ref. 14; it turns out that this relationship is obscured by the strong energy dependence of the proportionality constant already implicit in Eq. (2). Significant deviations from RMT are observed for large leads width (W of the order of the system size L). In particular the weak localization term decreases as W approaches L reaching a value much smaller than the RMT prediction. The weak localization term remains finite as L is increased.

The paper is organized as follows. Section II includes a description of our model of chaotic quantum dot and of the method we used to compute the current. The results are discussed in Sec. III. We first briefly consider the case of zero field, comparing our results with those derived from RMT. The results concerning the effects of Fermi energy, leads width, and dot size are presented and discussed thereafter. Again, comparison with RMT is highlighted. Section IV is devoted to summarize the conclusions of our work.

II. MODEL AND PROCEDURES

A. Model of quantum chaotic dot

Our model of a quantum chaotic dot is described by means of a tight-binding Hamiltonian with a single atomic orbital per lattice site,

$$\hat{H}=-\sum_{\langle m,n;m',n'\rangle} t_{m,n;m',n'}|m,n\rangle\langle m',n'|, \tag{6}$$

where $|m,n\rangle$ represents an atomic orbital on site (m,n). Indexes run from 1 to L, and the symbol $\langle\ \rangle$ denotes that the sum is restricted to the *existing* nearest neighbors of site (m,n). Using Landau's gauge the hopping integral is $t_{m,n;m',n'}=\exp\{2\pi i[m/(L-1)^2](\Phi/\Phi_0)\}$, for $m=m'$, and 1 otherwise. Therefore the difference between our Hamiltonian H and the one corresponding to an ideal $L\times L$ cluster on the square lattice is the absence of hopping to and from L sites chosen at random among the L^2 sites defining the lattice. A full discussion of the properties of this model for the case of a closed system and zero field can be found in Ref. 18.

B. Conductance

The conductance (measured in units of the quantum of conductance $G_0=e^2/h$) was computed by using the implementation of Kubo formula described in Ref. 21 (applications to mesoscopic systems can be found in Refs. 22 and 23). For a current propagating in the x direction, the static electrical conductivity is given by

$$G=-2\left(\frac{e^2}{h}\right)\mathrm{Tr}[(\hbar\hat{v}_x)\,\mathrm{Im}\,\hat{\mathcal{G}}(E)(\hbar\hat{v}_x)\,\mathrm{Im}\,\hat{\mathcal{G}}(E)], \tag{7}$$

where $\mathrm{Im}\,\hat{\mathcal{G}}(E)$ is obtained from the advanced and retarded Green functions:

$$\mathrm{Im}\,\hat{G}(E)=\frac{1}{2i}[\hat{\mathcal{G}}^R(E)-\hat{G}^A(E)], \tag{8}$$

and the velocity (current) operator $\hat{v}_x$ is related to the position operator $\hat{x}$ through the equation of motion $\hbar\hat{v}_x=[\hat{H},\hat{x}]$, $\hat{H}$ being the Hamiltonian.

Numerical calculations were carried out connecting quantum dots to semiinfinite leads of width W in the range $1-L$. The hopping integral inside the leads and between leads and dot at the contact sites is taken equal to that in the quantum dot (ballistic case). Assuming the validity of both the one-electron approximation and linear response, the exact form of the electric field does not change the value of G. An abrupt potential drop at one of the two junctions provides the simplest numerical implementation of the Kubo formula[21] since, in this case, the velocity operator has finite matrix elements on only two adjacent layers and Green functions are just needed for this restricted subset of sites. Assuming this potential drop to occur at the left contact (lc) side, the velocity operator can be explicitly written as

$$i\hbar v_x=-\sum_{j=1}^{W}(|lc,j\rangle\langle 1,j|-|1,j\rangle\langle lc,j|), \tag{9}$$

where ($|lc,j\rangle$ are the atomic orbitals at the left contact sites nearest neighbors to the dot.

Green functions are given by

$$[E\hat{I}-\hat{H}-\hat{\Sigma}_1(E)-\hat{\Sigma}_2(E)]\hat{G}(E)=\hat{I}, \tag{10}$$

where $\hat{\Sigma}_{1,2}(E)$ are the self-energies introduced by the two semi-infinite leads.[24] Most calculations were carried out by assuming that the magnetic field was zero outside the dot. Under this assumption the retarded self-energy due to the mode of wave vector k_y can be calculated explicitly:

$$\Sigma(E)=\frac{1}{2}(E-\epsilon(k_y)-i\sqrt{4-[E-\epsilon(k_y)]^2}), \tag{11}$$

for energies within its band $|E-\epsilon(k_y)|<2$, where $\epsilon(k_y)=2\cos(k_y)$ is the eigenenergy of the mode k_y which is quantized as $k_y=(n_{k_y}\pi)/(W+1)$, n_{k_y} being an integer from 1 to W. The transformation from the normal modes to the local tight–binding basis is obtained from the amplitudes of the normal modes, $\langle n|k_y\rangle=\sqrt{2/(W+1)}\sin(nk_y)$. Some calcula-

tions were done taking a magnetic field on the leads equal to that within the dot. For such cases the self-energy was calculated iterating Dyson's equation. If not specified, calculations discussed hereafter correspond to the case of no magnetic field in the leads.

C. Numerical procedures

Input/output leads were attached at opposite corners of the dot as follows: input lead connected from site (1,1) to site $(1,1+W)$, and output lead from site $(L,1)$ to site $(L,1+W)$. We have checked that changing the sites at which leads are attached does not qualitatively modify the results discussed here. The conductance was averaged over disorder realizations (local distribution of vacancies) and within selected energy ranges. The latter were chosen to fit the number of channels in the leads. More specifically, for leads with $N_{\rm ch}$ channels energy averages were done in the range

$$E \in [E_{N_{\rm ch}}, E_{N_{\rm ch}+1}], \tag{12}$$

for $N_{\rm ch}$ channels in the leads, where

$$E_n = -2\left(1+\cos\frac{\pi n}{W+1}\right). \tag{13}$$

Some calculations were also carried out at a fixed Fermi energy. In all cases averages were done over at least 1200 values of the conductance.

As remarked above we hereafter discuss the effects of the Fermi energy, size of the cavity, and leads width on the shape of the weak localization peak. The Fermi energy controls the number of open channels and thus the maximum conductance, while the leads width fixes (in the tight-binding model used here) the maximum number of channels. Thus $N_{\rm ch}$ can be tuned by either varying the Fermi energy or the leads width or both. Besides, the Fermi energy can further affect the peak shape as suggested by the results of Ref. 10 which show that the critical flux is a function of the density of states and the diffusion coefficient [see Eq. (2)] both energy-dependent magnitudes. The degree of opening of the cavity is controlled by the leads width. Presumably, this will also be an important factor as far as the applicability of RMT results is concerned. Finally the dot size will also likely affect the peak shape as indicated by Eq. (2).

III. RESULTS

A. Zero-field conductance

Figure 1 shows relative deviations of the conductance with respect to the RMT result [see Eq. (4)] for narrow and rather wide leads as a function of the dot size L. It is noted that for small W deviations are always smaller than 5%, and typically below 2%. The results fluctuate more appreciably for the narrower lead $(W=1)$ as expected.[23] Relative deviations from the RMT result are significantly larger for $W=9$ and 18. The results of Fig. 1 suggest that the difference with respect RMT is not a size effect. The larger deviation, and stronger variation in the explored range of L, observed for $N_{\rm ch}=W=9$ is likely a consequence of the important contribution that the center of the band $(E=0)$ has in that case. Both the center of the band and its bottom $(E=-4)$ show rather odd behaviors. In particular at $E=0$ no weak localization effect was observed (see below).

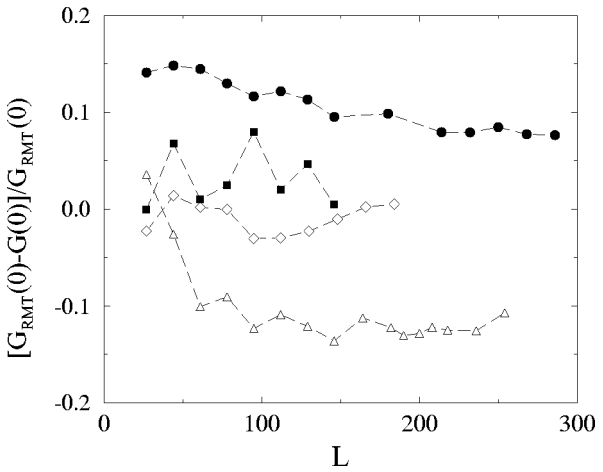

FIG. 1. Relative deviations of the numerical results for the zero-field conductance with respect to the RMT result versus dot size L. Leads of width W were attached at opposite corners of the dot. Chaoticity was induced by introducing L bulk vacancies (see text). Averages weere taken over 60 disorder realizations and 21 energies in the ranges corresponding to the number of channels $N_{\rm ch}$ in the leads (see text). The results correspond to $(W,N_{\rm ch})=(1,1)$: diamonds; (3,3): squares; (18,9): circles; and (9,9): triangles. The lines are guides to the eye.

The change in the zero-field conductance as the number of channels is varied, for fixed dot size, is illustrated in Fig. 2. The results for $N_{\rm ch}=W/2$ $(E=-2)$ can be accurately fitted by means of a straight line, as expected, although the

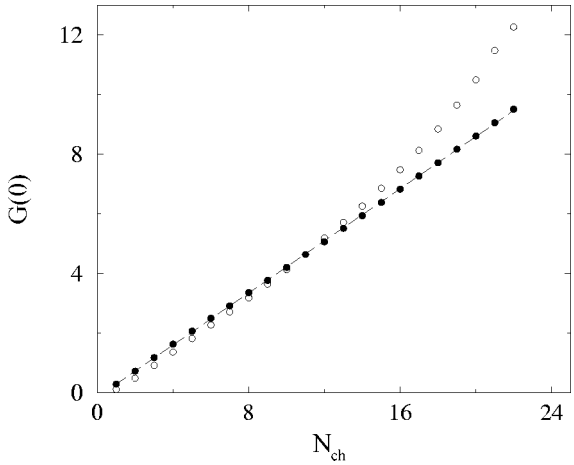

FIG. 2. Zero-field conductance $G(0)$ in units of the conductance quantum in dots of linear size $L=95$ versus the number of channels in the leads $N_{\rm ch}$. Leads of width $W=22$ (empty circles) and $W=2N_{\rm ch}$ (filled circles) were attached at opposite corners of the dot. Chaoticity was induced by introducing L bulk vacancies (see text). The results correspond to averages over 60 disorder realizations and 21 energies in the range corresponding the number of channels in the leads (see text). The straight line (broken curve) fitted to the results for $W=2N_{\rm ch}$ is $G(0)=0.44N_{\rm ch}-0.15$.

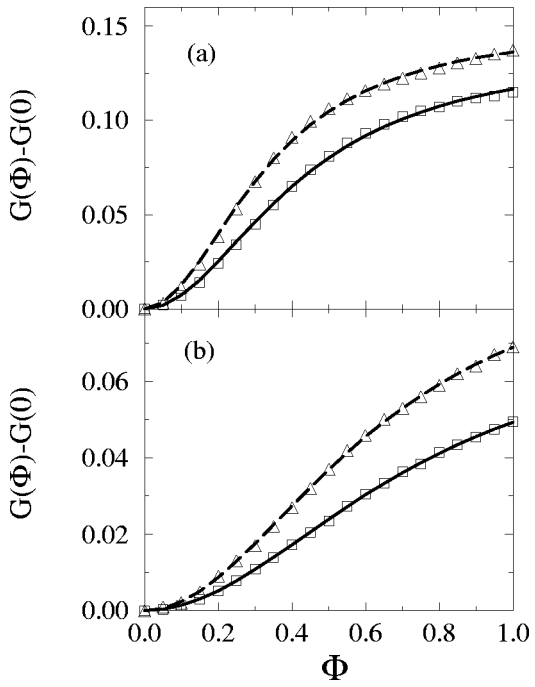

FIG. 3. Magnetoconductance as a function of the magnetic flux (in units of their respective quanta) in 78×78 chaotic cavities with leads of width $W=22$ (a) and 44 (b) attached at opposite corners of the dot, as discussed in the text. Chaoticity was induced by introducing $L=78$ bulk vacancies (see text). Averages were taken over 60 disorder realizations and 21 energies in the ranges corresponding to the number of channels N_{ch} in the leads. The numerical results correspond to $N_{ch}=4$ (triangles) and 12 (squares) and were fitted by means of Eq. (1) with the parameters reported in Table I.

slope is smaller than the RMT prediction [see caption of Fig. 2 and Eq. (4)]. The slope of the straight line varies with the ratio N_{ch}/W, or alternatively the average Fermi energy; for instance at $E=0$ ($N_{ch}=W$) it is actually larger than 0.5. For fixed leads width $W=22$ and a variable number of channels a large deviation with respect to a straight line is instead observed. This deviation increases with the number of channels and is likely due to the increasing contribution of the band center (note that, for fixed W, the number of channels is increased through an increase in the Fermi energy). Numerical results indicate that at the band center the conductance shows a much stronger dependence (increase) on the dot size that at any other energy within the band, probably due to the building up of the singularity in the density of states characteristic of the square lattice at that energy. These results suggest that if the N_{ch} dependence has to be investigated it is more reliable to work at a fixed N_{ch}/W ratio and vary the leads width.

B. Magnetoconductance: Weak localization

We first discuss the energy dependence of the critical flux and of the weak localization term. This was done by investigating rather large W and varying the number of channels in each lead. This is equivalent to vary the energy range over which the conductance was calculated (see above). Figure 3 depicts numerical results for cavities of linear size $L=78$ and leads of width $W=22$ (a) and 44 (b). The conductance was obtained by averaging over 60 disorder realizations and 21 energies in the ranges corresponding to the number of channels in the leads (see Sec. II C). The weak localization peak shows the expected behavior. The numerical results were fitted by means of Eq. (1) for fluxes in the range 0–1. At this stage it is worth noting that the conductance remains constant in a wide range of fluxes only for small W. For large W the conductance follows Eq. (1) in a rather narrow range of Φ (see below and Ref. 25). This deviation from the Lorentzian-like law hinders the fitting of the numerical results. The fitted parameters are reported in Table I. The parameters derived from RMT [Eqs. (3)–(5)] are also given in Table I. Equation (5) was used with $k=1$ as its explicit dependence on energy was not given in Ref. 14; this will suffice, however, to illustrate our point concerning the strong energy dependence of that constant. We first note that the weak localization term is smaller than the values predicted by RMT likely due to the large values of W (see below). However, the dependence of a/b on the number of channels is the correct one (it increases with N_{ch}) but for $W=44$ and $N_{ch}=28$. The latter deviation is a consequence of the increasing contribution of the band center.[26]

TABLE I. Fittings of numerical results such as those of Fig. 3 by means of Eq. (1) for 78×78 chaotic cavities with leads of width $W=22$ and 44 attached at opposite corners of the dot, as discussed in the text. Chaoticity was induced by introducing L vacancies within the bulk. The magnetoconductance was obtained by averaging over 60 disorder realizations and 21 energies in the ranges corresponding to the number of channels N_{ch} in the leads (see text). RMT results as obtained from Eqs. (3) and (5) with $k=1$ are also reported.

			Numerical		RMT	
W	N_{ch}	$G(0)$	b	a/b	b	a/b
22	4	1.32	5.62	0.137	0.88	0.22
	12	5.12	8.96	0.151	0.32	0.24
44	4	0.98	1.83	0.076	0.88	0.22
	12	4.62	2.46	0.097	0.32	0.24
	20	8.47	2.81	0.125	0.18	0.24
	28	12.87	4.73	0.091	0.14	0.25

The numerical results for parameter b show that it increases with the number of open channels, a behavior opposite to that given by RMT with $k=$const. This suggests that it cannot be safely concluded that the critical flux is proportional to the square root of the number of open channels, as, increasing the Fermi energy, not only increases N_{ch} but it also dramatically changes constant k in Eq. (5). The energy dependence of k already appears in the supersymmetric σ-model result.[10] We have checked that if the energy-dependent factor in Eq. (2) is included, the dependence of the RMT result on the number of channels can be reversed. The results are illustrated in Fig. 4 (the mean free path was calculated following the procedure of Refs. 13 and 22, see also Ref. 27). As shown in the caption, νD_0 increases with the number of channels slightly faster than linearly. This

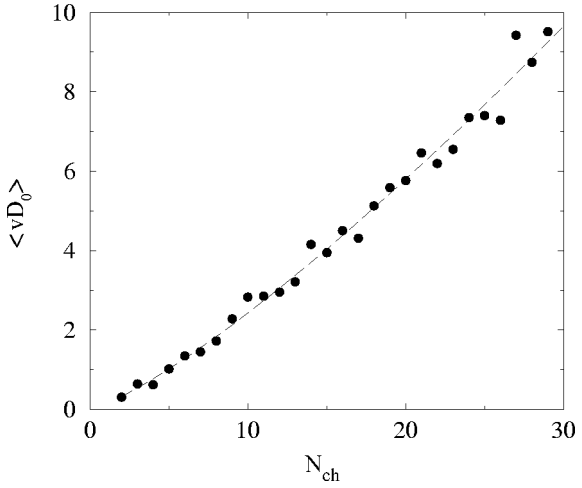

FIG. 4. Average of the product νD_0, where ν is the density of states and D_0 the diffusion coefficient, versus the number of channels in the leads. Energy averaging was carried out as $\langle \nu D_0 \rangle = \Sigma_{\mathbf{k}}(v_{\mathbf{k}} l_{\mathbf{k}})/(2L^2 \Delta E)$, where the sum runs over all $\mathbf{k}$ such that $E_{\mathbf{k}} \in [E_{N_{\rm ch}}, E_{N_{\rm ch}+1}]$ (see Sec. II C) $\Delta E = E_{N_{\rm ch}+1} - E_{N_{\rm ch}}$, and $v_{\mathbf{k}}$ and $l_{\mathbf{k}}$ are the electron velocity and mean free path, respectively. Further averaging was carried out over 20 realizations of disorder (L randomly distributed bulk vacancies). The results correspond to $L = 63$ and $W = 35$, while the fitted curve is $\langle \nu D_0 \rangle = 0.27 N_{\rm ch}^{1.26}$.

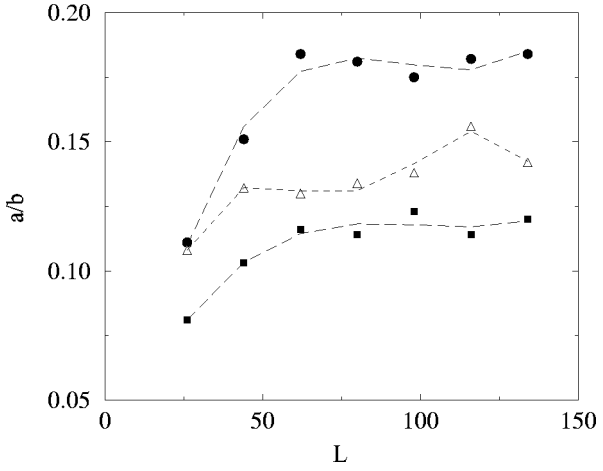

FIG. 5. Weak localization term [a/b in Eq. (1)] as a function of the dot size. Leads of width W were attached at opposite corners of the dot. Chaoticity was induced by introducing L bulk vacancies (see text). Averages were taken over 60 disorder realizations and 21 energies in the ranges corresponding to the number of channels $N_{\rm ch}$ in the leads (see text). The results correspond to $(W, N_{\rm ch}) = (10,5)$: circles; (2,1): triangles; and (1,1): squares. The lines are guides to the eye.

result is compatible with those reported in Table I (although no quantitative agreement is found). We note that, in some cases, the energy dependence of νD_0 may also give a constant b that decreases with the number of channels. In particular when $N_{\rm ch}$ becomes closer to W, the contribution of the band center increases and b begins to decrease due to the sharp decrease of the mean free path and the electron velocity near $E = 0$ (see, for instance, Ref. 27).

The effects of the dot size on the weak localization peak were investigated for L in the range of $L = 27$–137 and three combinations of $(W, N_{\rm ch})$. Averages were identical to those mentioned in the preceding paragraph. The results are depicted in Figs. 5 and 6. The weak localization term (a/b) shows a slight size dependence at small L, saturating for L approximately larger than 50 (see Fig. 5). This indicates that the smaller values of a/b obtained in our calculations, with respect to RMT, is probably not a size effect. The results for $(W, N_{\rm ch}) = (1,1)$ are slightly smaller than those for (2,1) surely due to the contribution of the band center in the first case. The results for (10,5) are larger than the other two, in agreement with RMT. On the other hand constant b increases with L as expected [see Eq. (2)]: the numerical results can be reasonably fitted by means of straight lines as shown in Fig. 6. The differences in the slopes is a consequence of the energy dependence discussed above.

In order to get rid as much as possible of the strong energy dependence of the weak localization peak, we have carried out the study of the effects of the leads width at a fixed energy. We have chosen $E = -2.001$ (away from the band center and bottom) which approximately correspond to $N_{\rm ch} = W/2$. We fixed the dot size at $L = 78$ and varied the leads width in the range $W = 4$–78. The results are shown in Figs. 7–9. The conductance versus the magnetic field for small and large W is depicted in Fig. 7. It is readily noted that both the weak localization term and constant b (or the inverse of the square root of the critical flux) sharply decrease with W. Although the results are nicely fitted by means of Eq. (1) the deviation of the numerical results with respect to that equation which occurs at large W (see above) is already observed for $W = 78$ (note that the fitting closely follows the numerical results only up to $\Phi \approx 1.5$). The decrease of b with $N_{\rm ch}$ is illustrated in Fig. 8 for $N_{\rm ch} = W/2$. The results can be satisfactorily fitted by means of the RMT result (see caption of Fig. 8). On the other hand the weak localization term depends on the leads width in a way that has not been previously anticipated (see Fig. 9). At small W (or number of channels) it increases as predicted by Eq. (3). However, beyond $W \approx 0.2L$ it begins to decrease sharply reaching a value slightly larger than 0.05 for $W = L$. The fact that this value is

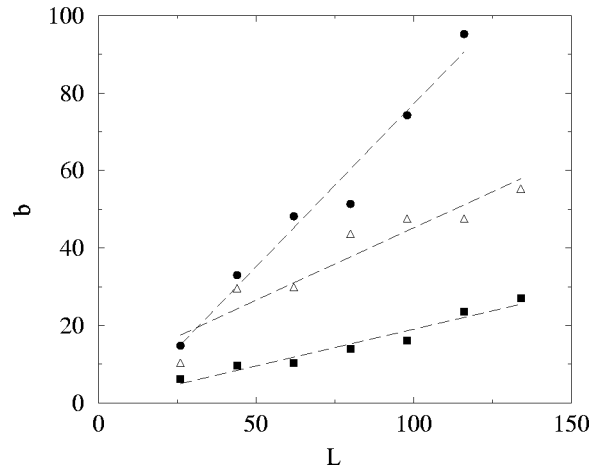

FIG. 6. Same as Fig. 5 for constant b in Eq. (1). The fitted straight lines are also shown.

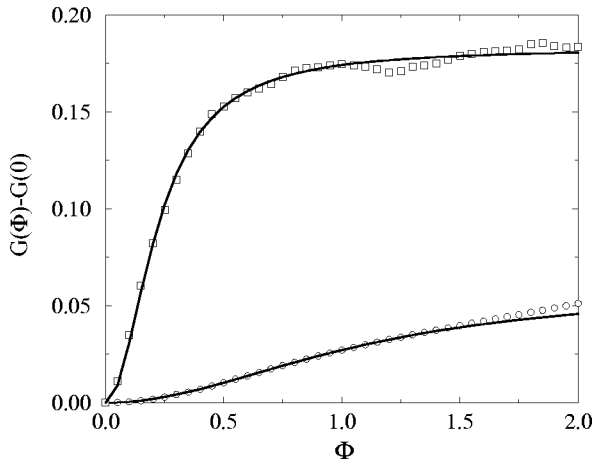

FIG. 7. Magnetoconductance as a function of the magnetic flux (in units of their respective quanta) in 78×78 chaotic cavities with leads of width $W=4$ and 78 (squares and circles, respectively) attached at opposite corners of the dot, as discussed in the text. Chaoticity was induced by introducing $L=78$ bulk vacancies (see text). The results correspond to averages over 1260 disorder realizations and a fixed energy $E=-2.001$ which roughly correspond to $N_{ch}=W/2$. The numerical results were fitted by means of Eq. (1)

well below the RMT prediction (0.25) suggests that a constant magnetic field within the dot does not introduce sufficient randomization to switch the system from the orthogonal to the unitary universality class. The effect is greatly enhanced as the system becomes more open (W increases).

To explore the possibility that the weak localization term vanishes in the large L limit and strongly open systems, we have calculated the magnetoconductance for $W=L$, $E=-2.001$ and L in the range 30–126. The numerical results for magnetic fluxes in the range 0–1 were fitted by means of Eq.

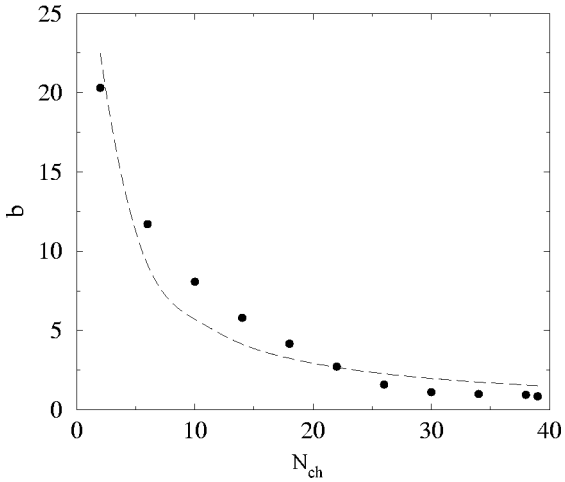

FIG. 8. Constant b in Eq. (1) as a function of the number of channels in the leads N_{ch}. Leads of width W were attached at opposite corners of dots of linear size $L=78$. Chaoticity was induced by introducing L bulk vacancies (see text). The results correspond to averages over 1260 disorder realizations, $W=4-78$ and a fixed energy $E=-2.001$ (which roughly corresponds to $N_{ch}=W/2$). The broken line is the RMT result obtained from Eq. (5) with $k=15$.

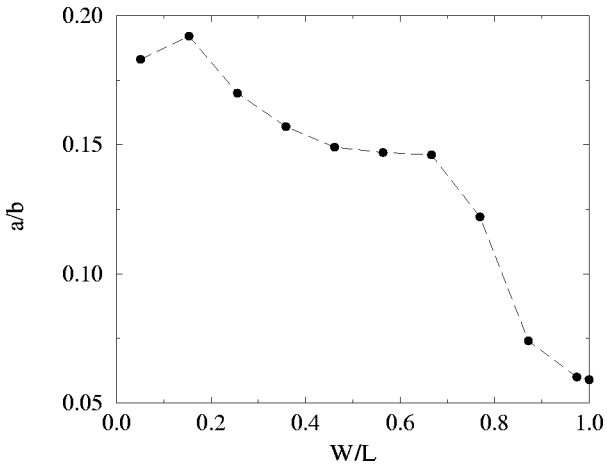

FIG. 9. Weak localization term [a/b in Eq. (1)] as a function of the leads width W. The leads were attached at opposite corners of dots of linear size $L=78$. Chaoticity was induced by introducing L bulk vacancies (see text). The results correspond to averages over 1260 disorder realizations, $W=4-78$ and a fixed energy $E=-2.001$. The line is a guide to the eye.

(1). Fitted parameters (b and a/b) are reported in Table II. The results clearly indicate that a/b does not vanish as L increases. The fact that b is almost independent of L is a consequence of the dependence of b on the ratio L/N_{ch} (note that by taking $W=L$ and a fixed energy the number of channels is proportional to L).

Finally we briefly discuss the effects of including the magnetic field in the leads, which would likely be stronger for wide leads and large fields. The results are illustrated in Fig. 10 for cavities of linear size $L=78$ and leads of width $W=L$. The two calculations (with or without field in the leads) give very similar results for fluxes up to $\Phi\approx6$, and differ only at a quantitative level for larger fluxes. A possible reason for this similarity is that as the Green's function of the whole system is calculated by means of Dyson equation, the effect of the field spreads over the leads up to some distance, even if no magnetic field was explicitly included in the leads.

TABLE II. Fittings of numerical results such as those of Fig. 3 by means of Eq. (1) for $L\times L$ chaotic cavities with leads of widths $W=L$ attached at opposite corners of the dot, as discussed in the text. Chaoticity was induced by introducing L vacancies within the bulk. The magnetoconductance was obtained by averaging over 1260 realizations of disorder and at a fixed energy $E=-2.001$ (which roughly corresponds to $N_{ch}=W/2$).

L	$G(0)$	b	a/b
30	6.50	0.66	0.058
42	9.34	0.89	0.051
54	12.19	0.91	0.056
66	15.04	0.76	0.070
78	17.91	0.85	0.059
102	23.65	0.98	0.053
114	26.49	0.87	0.054
126	29.37	0.88	0.047

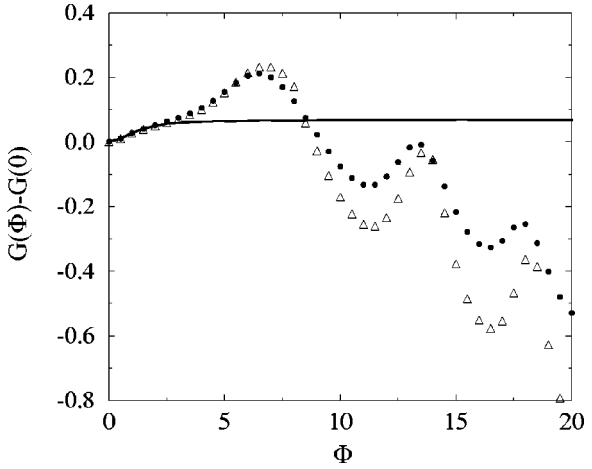

FIG. 10. Magnetoconductance as a function of the magnetic flux (in units of their respective quanta) in 78×78 chaotic cavities with leads of width $W=78$ attached at opposite corners of the dot, as discussed in the text. Chaoticity was induced by introducing $L=78$ bulk vacancies (see text). The results correspond to averages over 1260 disorder realizations, a fixed energy $E=-2.001$, and systems with (triangles) or without (circles) magnetic field in the leads. The continuous line is a fitting, by means of Eq. (1), of the numerical results for fluxes in the range 0–1.

This result has an important consequence: as from an experimental point of view neither of the two calculations is realistic (the leads will likely be partially located within the nonzero field region), the fact that these two limiting calculations give very similar results allows to carry either of the two rather safely. The results of Fig. 10 also illustrate a point raised above, namely, for large W (wide leads) the magnetoconductance follows Eq. (1) only for small magnetic fluxes.[25]

IV. CONCLUDING REMARKS

Summarizing, we have presented a detailed numerical study of the effects of Fermi energy, leads width, and dot size on the shape of the weak localization peak in quantum chaotic cavities. The study was carried out on a model that was recently proposed by us[18] which shows all the expected features of closed chaotic quantum billiards. Although the conclusions of our investigation qualitatively agree with most predictions of random matrix theory, some significant differences have to be highlighted. We first note that our results show that albeit the critical flux is proportional to the square root of the number of open channels, as predicted by RMT, the proportionality constant strongly depends on the Fermi energy in agreement with Efetov's analysis.[10] This introduces a model (system) dependence which makes theoretical (experimental) comparisons with RMT rather delicate. Our results clearly illustrate the size dependence of the critical flux, in particular $\Phi_c \propto 1/\sqrt{L}$, in agreement with Efetov results[10] and the RMT results reported in Refs. 16 and 17 (note that this size dependence was not found in a previously published RMT study, see Ref. 14). Finally, we have investigated the effects of the leads width concluding that the weak localization term sharply decreases with the ratio W/L reaching a value much smaller than the RMT prediction, although it probably remains finite in the infinite L limit.

ACKNOWLEDGMENTS

This work was supported in part by the Spanish CICYT (grants PB96-0085 and 1FD97–1358). Useful discussions with E. Cuevas and M. Ortuño are gratefully acknowledged.

[1] C.M. Marcus, A.J. Rimberg, R.M. Westervelt, P.F. Hopkins, and A.C. Gossard, Phys. Rev. Lett. **69**, 506 (1992).
[2] A.M. Chang, H.U. Baranger, L.N. Pfeiffer, and K.W. West, Phys. Rev. Lett. **73**, 2111 (1994).
[3] R.P. Taylor, R. Newbury, A.S. Sachrajda, Y. Feng, P.T. Coleridge, C. Dettmann, Ningjia Zhu, Hong Guo, A. Delage, P.J. Kelly, and Z. Wasilewski, Phys. Rev. Lett. **78**, 1952 (1997).
[4] A.S. Sachrajda, R. Ketzmerick, C. Gould, Y. Feng, P.J. Kelly, A. Delage, and Z. Wasilewski, Phys. Rev. Lett. **80**, 1948 (1998).
[5] H.U. Baranger, R.A. Jalabert, and A.D. Stone, Phys. Rev. Lett. **70**, 3876 (1993).
[6] X. Yang, H. Ishio, and J. Burgdörfer, Phys. Rev. B **52**, 8219 (1995).
[7] C.W.J. Beenakker, Rev. Mod. Phys. **69**, 731 (1997).
[8] T. Guhr, A. Müller-Groeling, and H.A. Weidenmüller, Phys. Rep. **299**, 189 (1998).
[9] P.A. Lee and T.V. Ramakrishnan, Rev. Mod. Phys. **57**, 287 (1985).
[10] K. Efetov, *Supersymmetry in Disorder and Chaos* (Cambridge University Press, Cambridge, 1997).
[11] Y.-C. Lai, R. Blümel, E. Ott, and C. Grebogi, Phys. Rev. Lett. **65**, 3491 (1992).
[12] R.A. Jalabert, H.U. Baranger, and A.D. Stone, Phys. Rev. Lett. **65**, 2442 (1990).
[13] E. Louis, E. Cuevas, J.A. Vergés, and M. Ortuño, Phys. Rev. B **56**, 2120 (1997).
[14] Z. Pluhar, H.A. Weidenmüller, J.A. Zuk, and C.H. Lewenkopf, Phys. Rev. Lett. **73**, 2115 (1994); **74**, 1258 (1995).
[15] H.U. Baranger and P.A. Mello, Phys. Rev. Lett. **73**, 142 (1994).
[16] K.M. Frahm and J.-L. Pichard, J. Phys. I **5**, 877 (1995).
[17] Z. Pluhar, H.A. Weidenmüller, J.A. Zuk, C.H. Lewenkopf, and F.J. Wegner, Ann. Phys. (N.Y.) **243**, 1 (1995).
[18] J.A. Vergés and E. Louis, Phys. Rev. E **59**, R3803 (1999); E. Louis, J.A. Vergés, and E. Cuevas, *ibid.* **60**, 391 (1999).
[19] E. Cuevas, E. Louis, and J.A. Vergés, Phys. Rev. Lett. **77**, 1970 (1996).
[20] Y.M. Blanter, A.D. Mirlin, and B.A. Muzykantskii, Phys. Rev. Lett. **80**, 4161 (1998); V. Tripathi and D.E. Khmelnitskii, Phys. Rev. B **58**, 4161 (1998).
[21] J.A. Vergés, Comput. Phys. Commun. **118**, 71 (1999).

[22] E. Cuevas, E. Louis, M. Ortuño, and J.A. Vergés, Phys. Rev. B **56**, 15 853 (1997); J.A. Vergés, E. Cuevas, M. Ortuño, and E. Louis, *ibid.* **58**, R10 143 (1998).

[23] E. Louis and J.A. Vergés, Phys. Rev. B **61**, 13 014 (2000).

[24] S. Datta, *Electronic Transport in Mesoscopic Systems* (Cambridge University Press, Cambridge, 1995).

[25] At large fields the behavior of the conductance may strongly depend on the model. For bulk disorder (the case considered here) the contribution of edge states is strongly reduced and, as a consequence, the conductance decreases while in the case of surface disorder it increases as a function of the magnetic flux (until a maximum flux at which edge states begin to depopulate). However, this difference is unimportant in the present case as we are interested in the low-field behavior.

[26] Just at the band center the results indicate that the magnetoconductance decreases as a function of the flux, i.e., there is no weak localization effect (see also Sec. III A). Due to computing limitations we have not been able to check whether this result is a size effect.

[27] P. Sheng, *Introduction to Wave Scattering, Localization, and Mesoscopic Phenomena* (Academic Press, New York, 1995).